Analysis of the Crystallization Kinetics of Lysozyme using a Model with Polynuclear Growth Mechanism

Yasuo Bessho, Mitsuo Ataka, Michihiko Asai,* and Tatsuo Katsura
National Institute of Bioscience and Human Technology, 1–1 Higashi, Tsukuba 305, Japan

ABSTRACT A differential equation model with a polynuclear growth mechanism was formulated for a theoretical understanding of protein crystallization. The model equation contains two parameters characterizing nucleation and growth: the number of protein molecules constituting a critical nucleus and the order of growth kinetics. This model was applied successfully to explain the experimental data on the protein concentration changes due to nucleation and crystal growth of tetragonal and orthorhombic hen egg-white lysozyme. It was shown that the critical nucleus most probably consists of three or four molecules. The range and extent of the validity of the present model and analysis are discussed.

INTRODUCTION

The technique of protein crystallography for structure determination has advanced greatly in recent years and, in many cases, preparation of suitable crystals has become the rate-limiting step (Lesk, 1991). The study of the protein crystallization mechanism and kinetics is important in this respect. Furthermore, it may contribute to the further understanding of protein interaction and association of biological significance.

We investigated previously the kinetics of protein crystallization as a process in which nucleation and growth proceed simultaneously and analyzed it (Ataka and Asai, 1990; Elgersma et al., 1992) by applying a theory of protein self-assembly (Oosawa and Asakura, 1975). The theory originally concerns nucleation and one-dimensional polymerization of protein and was used to elucidate actin polymerization.

Our experiments were executed batch-wise for supersaturated solutions of hen egg-white lysozyme as a model protein with different initial concentrations at fixed temperature and pH, and the concentration changes on crystallization were measured using ultraviolet spectroscopy. For the crystallization curves thus obtained, a linear relation was found between the initial concentration minus solubility and the half-reduction time in logarithmic scales. This linearity was consistent with the prediction of the theory of protein self-assembly. According to the theory, the number of monomers constituting a critical nucleus (the smallest nucleus from which a polymer or crystal begins to grow) could be obtained from the slope of this line. The estimated numbers were three to five under the experimental conditions adopted.

Although the application of the theory was apparently successful, a point that remained to be considered was that the growth rate might depend on the crystal size for three-dimensional crystallization in contrast to simple one-dimensional polymerization. Furthermore, electron micrographs that suggest the polynuclear growth (PNG) mechanism of lysozyme crystallization were obtained recently (Durbin and Feher, 1990). These points must be taken into account to establish a clear picture of the crystal growth of this protein.

In this paper, we analyze the crystallization kinetics of lysozyme, adopting a differential equation model of simultaneously proceeding nucleation and three-dimensional growth with a PNG mechanism. The analysis enables us to estimate both the number of the monomers constituting the critical nucleus and the order of growth kinetics.

FORMULATION OF THE MODEL

A differential equation system describing nucleation and three-dimensional crystal growth was formulated by Nielsen (1964). According to the formulation, nucleation kinetics is given by

$$dm/dt = k_1 c^i, \tag{1}$$

where m is the number concentration of nucleus, c the concentration of monomer, and k_1 the rate constant for nucleation. The exponent i represents the number of monomers constituting a critical nucleus and is assumed to remain constant, irrespective of c. On the other hand, growth kinetics with a PNG mechanism is represented as

$$dr_{\tau,t}/dt = k_2 c^p \tag{2}$$

with

$$c = c_0 - (\omega/\nu) \int_0^t (dm/d\tau) r_{\tau,t}^3 \, d\tau, \tag{3}$$

where $r_{\tau,t}$ is the radius or edge length of the crystals nucleated at time τ and grew until time t and k_2 the rate constant for growth. The exponent p represents the order of growth kinetics assumed to remain constant as i. Equation 3 represents the conservation of the molecules per unit volume of the solution, where c_0 is the initial concentration of monomer, ω

Received for publication 22 March 1993 and in final form 9 November 1993.
Address reprint requests to Yasuo Bessho.
*Present address: National Institute of Materials and Chemical Research, 1–1 Higashi, Tsukuba 305, Japan.

0006-3495/94/02/310/04 $2.00

the shape factor of the crystals, i.e., $\omega r_{\tau,t}^3$ equals the volume of a crystal nucleated at time τ, and v the specific volume (volume per unit mass) of the crystals. When $p = 1$, Eqs. 2 and 3 represent simple adhesive growth kinetics without surface nucleation.

We considered the details of the growth mechanism by surface nucleation. The surface nucleation rate J is given by the same form as Eq. 1:

$$J = k_3 c^{i'}, \tag{4}$$

where i' is the number of monomers constituting a critical surface nucleus and k_3 a rate constant. We also assume that the linear growth rate of the nucleated surface layers V is given by:

$$V = k_4 c^j, \tag{5}$$

where positive integer j is the order of the growth of the nucleated surface layers representing the adhesion of cooperative j monomers or of j mers, and k_4 a rate constant.

The general expression for the linear growth rate of a crystal with a PNG mechanism with sufficiently large numbers of surface nuclei is given by

$$R_p = h\alpha(bJV^2)^{1/3}, \tag{6}$$

where b is the shape factor and h the step height of the nucleated surface layers, and α a constant (Obretenov et al., 1989). Using Eqs. 4 and 5, Eq. 6 becomes

$$R_p = h\alpha(bk_3k_4^2)^{1/3}c^{(i'+2j)/3}. \tag{7}$$

R_p being equivalent to $dr_{\tau,t}/dt$ (Eq. 2), we obtain the relation

$$p = (i' + 2j)/3. \tag{8}$$

FEATURES OF THE MODEL

A distinctive feature of the model, indispensable to the explanation and analysis of our experimental data, is that the following scaling relation holds (Nielsen, 1964) for any pair of solutions with different values of k_1, k_2, and c_0:

$$T = (k_1/K_1)^{1/4}(k_2/K_2)^{3/4}(c_0/C_0)^{(i+3p-1)/4}t. \tag{9}$$

Here we suppose k_1 and k_2 to be invariable for analyzing the experimental data obtained under fixed pH and temperature. When $K_1 = k_1$, $K_2 = k_2$, and $C_0 = 1$, Eq. 9 becomes

$$T = c_0^{\gamma}t \tag{10}$$

with

$$\gamma = (i + 3p - 1)/4. \tag{11}$$

From Eq. 10, we get the relation

$$\log T = \gamma \log c_0 + \log t. \tag{12}$$

Equation 12 means that the solution which represents the crystallization curve with the initial concentration c_0 has the same shape as that with $C_0 = 1$, and the former can be superimposed on the latter by the translation $\gamma \log c_0$ along the $\log t$ axis.

If we introduce $t_{1/2}$ and $T_{1/2}$ for the times when the concentrations reduce to the halves of the respective initial concentrations c_0 and 1, the relation between $\log t_{1/2}$ and $\log c_0$ is obtained from Eq. 12:

$$\log t_{1/2} = -\gamma \log c_0 + \log T_{1/2}. \tag{13}$$

By applying Eq. 13 to the experimental crystallization curves with various c_0, we can estimate the value of γ, which is defined by the exponents characterizing nucleation and growth (see Eq. 11).

Another feature of the model found by numerical computation, which provides a simple viewpoint for the interpretation of the experimental data, is that the shapes of the crystallization curves are virtually determined by p alone and independent of i.

ANALYSIS OF THE EXPERIMENTAL DATA

We can apply the model formulated above to the experimental data previously obtained: $Ortho_{4.6}$ (35°C, pH = 4.6, orthorhombic), $Ortho_{6.0}$ (35°C, pH = 6.0, orthorhombic), and $Tetra_{6.0}$ (5°C, pH = 6.0, tetragonal) (Elgersma et al., 1992). In the analysis below, we use Eqs. 1–3 with the actual concentration minus solubility ($c - c_s$) in place of c. This modification is necessary to satisfy the requirement that the driving force of the crystallization must be 0 when $c = c_s$.

The experimental data and the best fit theoretical curves are shown in Fig. 1. The experimental crystallization curves with various initial concentrations have a similar shape and can be superimposed on each other by the translation along the $\log t$ axis. The present model can certainly explain such a feature as noted in the previous section. On the other hand, the crystallization curves for different temperature or pH exhibit different shapes. As also mentioned above, the model ascribes this feature to a differing value of p and, accordingly, to the detailed mechanism of PNG, not to the nucleation kinetics.

The linear relations between $\log t_{1/2}$ and $\log (c_0 - c_s)$ represented by Eq. 13 were really observed on the experimental data as already mentioned in the Introduction and are shown in Fig. 2. The estimated values of γ were: 2.0 for $Ortho_{4.6}$, 1.5 for $Ortho_{6.0}$, and 2.4 for $Tetra_{6.0}$. On the other hand, theoretical values of p and γ are restricted by the requirement that i', j, and i should be positive integers according to Eqs. 8 and 11. Possible combinations of $(i, p(i', j), i', j)$ to explain the experimentally obtained values of γ are shown in Table 1.

By numerical computation, we obtained the theoretical curves corresponding to all possible pairs of i and p compatible with experimental γ. For each pair of i and p, the time scales of the theoretical curves with different c_0 were optimized as a whole by minimizing the standard deviation from the experimental data, where $k_1^{1/4}\,k_2^{3/4}$ was taken as the fitting parameter (see Eq. 9). The standard deviation data for different i and p are presented in Table 2. The (i, p) values for the best fit curves with the minimum standard deviations are (3, 2) for $Ortho_{4.6}$, (3, 4/3) for $Ortho_{6.0}$, and (4, 7/3) for

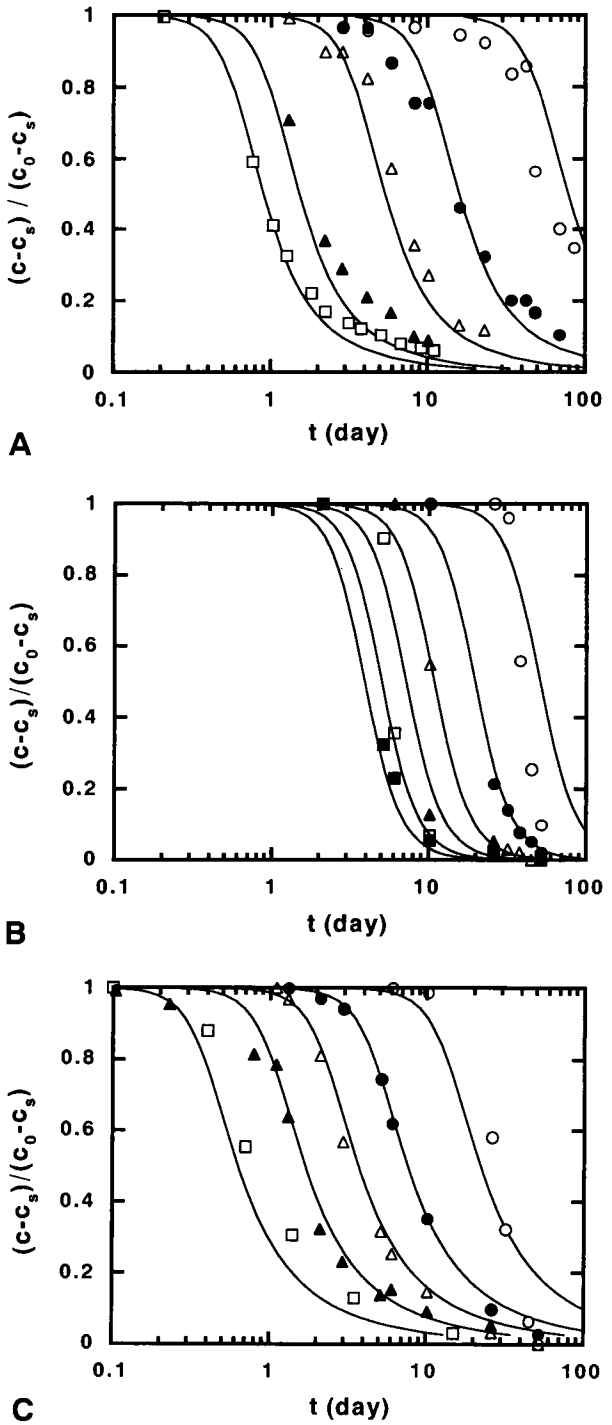

FIGURE 1 Crystallization data of hen-egg white lysozyme and the best fit theoretical curves with the minimum standard deviation. The experiments were carried out batch-wise in water with 3.0 wt % NaCl and without buffer for various initial concentrations (c_0). The concentration of lysozyme in solution was determined using an ultraviolet spectrophotometer (Cary 14D or Shimadzu MPS-2000). The *vertical axis* shows normalized supersaturation concentration, where c_s is solubility, and the *horizontal axis* represents time (in days). (*A*) $Ortho_{4.6}$ (35°C, pH = 4.6, orthorhombic): c_s, 1.15 (wt %); c_0: 9.71 (□), 7.73 (▲), 4.66 (△), 3.19 (●), 2.07 (○); (*i*, *p*), (3, 2). (*B*) $Ortho_{6.0}$ (35°C, pH = 6.0, orthorhombic): c_s, 0.93; c_0: 6.57 (■), 5.71 (□), 4.69 (▲), 3.79 (△), 2.85 (●), 1.95 (○); (*i*, *p*), (3, 4/3). (*C*) $Tetra_{6.0}$ (5°C, pH = 6.0, tetragonal): c_s, 0.17; c_0; 2.10 (□), 1.47 (▲), 1.12 (△), 0.88 (●), 0.63 (○); (*i*, *p*), (4, 7/3). The standard deviation data for different (*i*, *p*) are shown in Table 2.

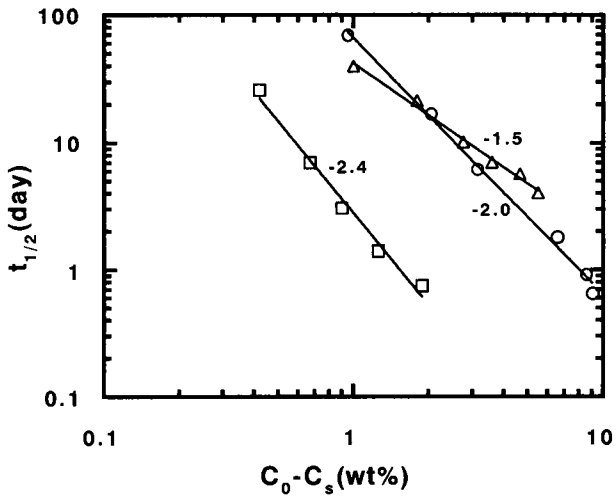

FIGURE 2 Relation between $t_{1/2}$ and $c_0 - c_s$ in log scale for different experimental conditions. The slopes determined by the least squares fit are indicated. (○) $Ortho_{4.6}$ (35°C, pH = 4.6); (△) $Ortho_{6.0}$ (35°C, pH = 6.0); (□) $Tetra_{6.0}$ (5°C, pH = 6.0).

TABLE 1 Possible combinations of (*i*, *p*(*i'*, *j*), *i'*, *j*)

$\gamma(i, p)$	i	$p(i', j)$	i'	j
2 ($Ortho_{4.6}$)	3	2	2	2
	3	2	4	1
	4	5/3	3	1
	5	4/3	2	1
	6	1	1	1
3/2 ($Ortho_{6.0}$)	3	4/3	2	1
	4	1	1	1
5/2 ($Tetra_{6.0}$)	3	8/3	2	3
	3	8/3	4	2
	3	8/3	6	1
	4	7/3	3	2
	4	7/3	5	1
	5	2	2	2
	5	2	4	1
	6	5/3	3	1
	7	4/3	2	1
	8	1	1	1

$Tetra_{6.0}$. The corresponding (i', j) are (2, 2) and (4, 1) for $Ortho_{4.6}$, (2, 1) for $Ortho_{6.0}$, and (3, 2) and (5, 1) for $Tetra_{6.0}$ (see Table 1).

DISCUSSION

Using a three-dimensional growth model with a PNG mechanism we estimated two important parameters characterizing the crystallization of lysozyme: the size of the critical nucleus (i) and the order of growth kinetics (p).

The most probable size of the critical nucleus was estimated as three or four, depending on temperature and pH. This result is similar to that obtained previously using the theory of protein self-assembly. We can attribute this to the oppositely operative terms of Eq. 11, i.e., $i/4$ and $(3p - 1)/4$, the sum of which is given experimentally, by comparing with the corresponding expression $\gamma = i/2$ in the previous analysis: the estimation of i did not become larger because of the

TABLE 2 Standard deviations for theoretical curves

	i	p	$(\omega/v)^{1/4}k_1^{1/4}k_2^{3/4}$	Standard deviation
$Ortho_{4.6}$	3	2	0.0552	0.0789
	4	5/3	0.0510	0.0976
	5	4/3	0.0471	0.1187
	6	1	0.0440	0.1401
$Ortho_{6.0}$	3	4/3	0.0620	0.1410
	4	1	0.0575	0.1439
$Tetra_{6.0}$	3	8/3	1.290	0.0715
	4	7/3	1.203	0.0635
	5	2	1.119	0.0636
	6	5/3	1.027	0.0727
	7	4/3	0.940	0.0884
	8	1	0.855	0.1055

second term. It is interesting that the estimated critical nuclear size of three or four also coincides with those for the polymerization of actin and flagellin (Oosawa and Asakura, 1975), although the coincidence may not necessarily imply the similarity of the nucleation mechanism.

According to the generally accepted view for nucleation, the critical nuclear size is defined by the maximum point of the free energy function composed of two parts representing negative volume energy and positive surface energy. The invariance of the critical nuclear size (i), which was supposed in the present model and justified by the linear relation between log c_0 and log $t_{1/2}$, means that the maximum point of the free energy function for nucleation is almost invariable in such a wide range of concentrations. Another reason for the invariance may be that the free energy of a nucleus composed of only a few monomers varies in relatively large degree even when only one monomer is added or removed and, as a result, the critical nuclear size is not sensitive to the change of the free energy function.

The order of growth kinetics (p) was estimated from the shape of the crystallization curves under the condition of Eq. 8, in which positive integers i' and j represent the size of the critical surface nucleus and the order of the growth from the surface nucleus, respectively. For $Ortho_{6.0}$, the possible pair of (i', j) corresponding to p for the best fit curves is unique, whereas in the cases of $Ortho_{4.6}$ and $Tetra_{6.0}$ it is not uniquely determined (see Table 1). However, if we adopt the assumption that a surface nucleus is more stable than a nucleus of the same size, possible (i', j) is uniquely determined also in these cases: (2, 2) for $Ortho_{4.6}$ and (3, 2) for $Tetra_{6.0}$. The elementary process of the surface nuclear growth with $j = 2$ can be either the cooperative interaction between two monomers or dimer-based adhesion.

The rate constants for growth may be different among different faces of the same crystal. For crystals with three different rate constants k_{21}, k_{22}, and k_{23}, it can be shown easily that the present model and analysis are valid with the substitution

$$k_2 = (k_{21}k_{22}k_{23})^{1/3}. \quad (14)$$

It is also possible that the orders of growth kinetics are different among different faces. In such a case, a crystallization curve is defined by the sum of the growth on different faces and p is estimated from its shape by the curve-fitting procedure. Therefore, estimated p can be considered to take an average value of real parameters for different faces and still provides useful information about the growth mechanism.

While the experimental data $Ortho_{4.6}$ and $Tetra_{6.0}$ agree well with the optimized theoretical curves, $Ortho_{6.0}$ shows some deviations characterized by the longer latent periods and subsequent steeper slopes in log t scale (Fig. 1). Unfortunately, the experimental data points of $Ortho_{6.0}$ seem to be insufficient, partly due to the steep decline of the concentration to provide reliable discussion about the deviations. However, it is possible that the PNG model, which supposes sufficiently frequent occurrence of surface nucleation, was not very appropriate for $Ortho_{6.0}$ and that the linear growth rates for small crystals were depressed. The characteristics of the data are apparently explained from this point of view.

On the other hand, the crystallization curves of the data $Tetra_{4.0}$ (5°C, pH = 4.0, tetragonal), which we have not addressed in this paper, have too moderate slopes in log t scale to be explained by the present model. Using numerical computation, we have found that this character can be reproduced by supposing a diffusion-controlled growth equation in place of Eq. 2. Further investigation is necessary to ascertain whether these observations are valid.

The study of the simultaneously occurring nucleation and crystal growth system of lysozyme has provided useful information, in particular about critical nuclei and surface critical nuclei, both of which are difficult to observe directly because they begin to grow at the moments when they are created. Application of the present model to other protein crystallization systems is also promising, since no particular assumption for lysozyme crystallization is supposed herein. Combination with other experimental methods such as dynamic light scattering and laser Michelson interferometry (Vekilov et al., 1993) will allow deeper understanding about the crystallization of lysozyme and other proteins.

We thank Dr. F. Oosawa for valuable discussions.

REFERENCES

Ataka, M., and M. Asai. 1990. Analysis of the nucleation and crystal growth kinetics of lysozyme by a theory of self-assembly. *Biophys. J.* 58: 807–811.

Durbin, S. D., and G. Feher. 1990. Studies of crystal growth mechanisms of proteins by electron microscopy. *J. Mol. Biol.* 212:763–774.

Elgersma, A. V., M. Ataka, and T. Katsura. 1992. Kinetic studies on the growth of three crystal forms of lysozyme based on the measurement of protein and Cl^- concentration changes. *J. Cryst. Growth.* 122:31–40.

Lesk, A. M. 1991. Protein Architecture. IRL Press, Oxford, UK.

Nielsen, A. E. 1964. Kinetics of Precipitation. Pergamon Press, Oxford, UK.

Obretenov, W., D. Kashchiev, and V. Bostanov. 1989. Unified description of the rate of nucleation-mediated crystal growth. *J. Cryst. Growth.* 96: 843–848.

Oosawa, F., and S. Asakura. 1975. Thermodynamics of the Polymerization of Protein. Academic Press, New York.

Vekilov, P. G., M. Ataka, and T. Katsura. 1993. Laser Michelson interferometry investigation of protein crystal growth. *J. Cryst. Growth.* 130: 317–320.